PROCEEDINGS OF SPIE

SPIEDigitalLibrary.org/conference-proceedings-of-spie

The ASTRO-H (Hitomi) x-ray astronomy satellite

Tadayuki Takahashi, Motohide Kokubun, Kazuhisa Mitsuda, Richard Kelley, Takaya Ohashi, et al.

Tadayuki Takahashi, Motohide Kokubun, Kazuhisa Mitsuda, Richard Kelley, Takaya Ohashi, Felix Aharonian, Hiroki Akamatsu, Fumie Akimoto, Steve Allen, Naohisa Anabuki, Lorella Angelini, Keith Arnaud, Makoto Asai, Marc Audard, Hisamitsu Awaki, Magnus Axelsson, Philipp Azzarello, Chris Baluta, Aya Bamba, Nobutaka Bando, Marshall Bautz, Thomas Bialas, Roger Blandford, Kevin Boyce, Laura Brenneman, Greg Brown, Esra Bulbul, Edward Cackett, Edgar Canavan, Maria Chernyakova, Meng Chiao, Paolo Coppi, Elisa Costantini, Jelle de Plaa, Jan-Willem den Herder, Michael DiPirro, Chris Done, Tadayasu Dotani, John Doty, Ken Ebisawa, Megan Eckart, Teruaki Enoto, Yuichiro Ezoe, Andrew Fabian, Carlo Ferrigno, Adam Foster, Ryuichi Fujimoto, Yasushi Fukazawa, Akihiro Furuzawa, Massimiliano Galeazzi, Luigi Gallo, Poshak Gandhi, Kirk Gilmore, Margherita Giustini, Andrea Goldwurm, Liyi Gu, Matteo Guainazzi, Daniel Haas, Yoshito Haba, Kouichi Hagino, Kenji Hamaguchi, Atsushi Harayama, Ilana Harrus, Isamu Hatsukade, Takayuki Hayashi, Katsuhiro Hayashi, Kiyoshi Hayashida, Junko Hiraga, Kazuyuki Hirose, Ann Hornschemeier, Akio Hoshino, John Hughes, Yuto Ichinohe, Ryo Iizuka, Yoshiyuki Inoue, Hajime Inoue, Kazunori Ishibashi, Manabu Ishida, Kumi Ishikawa, Kosei Ishimura, Yoshitaka Ishisaki, Masayuki Itoh, Naoko Iwata, Naoko Iyomoto, Chris Jewell, Jelle Kaastra, Timothy Kallman, Tuneyoshi Kamae, Erin Kara, Jun Kataoka, Satoru Katsuda, Junichiro Katsuta, Madoka Kawaharada, Nobuyuki Kawai, Taro Kawano, Shigeo Kawasaki, Dmitry Khangulyan, Caroline Kilbourne, Mark Kimball, Ashley King, Takao Kitaguchi, Shunji Kitamoto, Tetsu Kitayama, Takayoshi Kohmura, Tatsuro Kosaka, Alex Koujelev, Katsuji Koyama, Shu Koyama, Peter Kretschmar, Hans Krimm, Aya Kubota, Hideyo Kunieda, Philippe Laurent, François Lebrun, Shiu-Huang Lee, Maurice Leutenegger, Olivier Limousin, Michael Loewenstein, Knox Long, David Lumb, Grzegorz Madejski, Yoshitomo Maeda, Daniel Maier, Kazuo Makishima, Maxim Markevitch, Candace Masters, Hironori Matsumoto, Kyoko Matsushita, Dan McCammon, Daniel McGuinness, Brian McNamara, Missagh Mehdipour, Joseph Miko, Jon Miller, Eric Miller, Shin Mineshige, Kenji Minesugi, Ikuyuki Mitsuishi, Takuya Miyazawa, Tsunefumi Mizuno, Koji Mori, Hideyuki Mori, Franco Moroso, Harvey Moseley, Theodore Muench, Koji Mukai, Hiroshi Murakami, Toshio Murakami, Richard Mushotzky, Housei Nagano, Ryo Nagino, Takao Nakagawa, Hiroshi Nakajima, Takeshi Nakamori, Toshio Nakano, Shinya Nakashima, Kazuhiro Nakazawa, Yoshiharu Namba, Chikara Natsukari, Yusuke Nishioka, Masayoshi Nobukawa, Kumiko Nobukawa, Hirofumi Noda, Masaharu Nomachi, Steve O'Dell, Hirokazu Odaka, Hiroyuki Ogawa, Mina Ogawa, Keiji Ogi, Masanori Ohno, Masayuki Ohta, Takashi Okajima, Atsushi Okamoto, Tsuyoshi Okazaki, Naomi Ota, Masanobu Ozaki, Frederik Paerels, Stéphane Paltani, Arvind Parmar, Robert Petre, Ciro Pinto, Martin Pohl, James Pontius, F. Scott Porter, Katja Pottschmidt, Brian Ramsey, Christopher Reynolds, Helen Russell, Samar Safi-Harb, Shinya Saito, Shin-ichiro Sakai, Kazuhiro Sakai, Hiroaki Sameshima, Toru Sasaki, Goro Sato, Yoichi Sato, Kosuke Sato, Rie Sato, Makoto Sawada, Norbert Schartel, Peter Serlemitsos, Hiromi Seta, Yasuko Shibano, Maki Shida, Megumi Shidatsu, Takanobu Shimada, Keisuke Shinozaki, Peter Shirron, Aurora Simionescu, Cynthia Simmons, Randall Smith, Gary Sneiderman, Yang Soong, Łukasz Stawarz, Yasuharu Sugawara, Hiroyuki Sugita, Satoshi Sugita, Andrew Szymkowiak, Hiroyasu Tajima, Hiromitsu Takahashi, Shin'ichiro Takeda, Yoh Takei, Toru Tamagawa, Takayuki Tamura, Keisuke Tamura, Takaaki Tanaka, Yasuo Tanaka, Yasuyuki Tanaka, Makoto Tashiro, Yuzuru Tawara, Yukikatsu Terada, Yuichi Terashima, Francesco Tombesi, Hiroshi Tomida, Yohko Tsuboi, Masahiro Tsujimoto, Hiroshi Tsunemi, Takeshi Tsuru, Hiroyuki Uchida, Yasunobu Uchiyama, Hideki Uchiyama, Yoshihiro Ueda, Shutaro Ueda, Shiro Ueno, Shin'ichiro Uno, Meg Urry, Eugenio Ursino, Cor de Vries, Atsushi Wada, Shin Watanabe, Tomomi Watanabe, Norbert Werner, Daniel Wik, Dan Wilkins, Brian Williams, Takahiro Yamada, Shinya Yamada, Hiroya Yamaguchi, Kazutaka Yamaoka, Noriko Yamasaki, Makoto Yamauchi, Shigeo Yamauchi, Tahir Yaqoob, Yoichi Yatsu, Daisuke Yonetoku, Atsumasa Yoshida, Takayuki Yuasa, Irina Zhuravleva, Abderahmen Zoghbi, "The ASTRO-H (Hitomi) x-ray astronomy satellite," Proc. SPIE 9905, Space Telescopes and Instrumentation 2016: Ultraviolet to Gamma Ray, 99050U (20 July 2016); doi: 10.1117/12.2232379

Event: SPIE Astronomical Telescopes + Instrumentation, 2016, Edinburgh, United Kingdom

The ASTRO-H (Hitomi) X-ray Astronomy Satellite

Tadayuki Takahashi[a], Motohide Kokubun[a], Kazuhisa Mitsuda[a], Richard Kelley[b], Takaya Ohashi[c], Felix Aharonian[d], Hiroki Akamatsu[e], Fumie Akimoto[f], Steve Allen[g], Naohisa Anabuki[h], Lorella Angelini[b], Keith Arnaud[i], Makoto Asai[g], Marc Audard[j], Hisamitsu Awaki[k], Magnus Axelsson[c], Philipp Azzarello[j], Chris Baluta[a], Aya Bamba[l], Nobutaka Bando[a], Marshall Bautz[m], Thomas Bialas[b], Roger Blandford[g], Kevin Boyce[b], Laura Brenneman[n], Greg Brown[o], Esra Bulbul[m], Edward Cackett[p], Edgar Canavan[b], Maria Chernyakova[d], Meng Chiao[b], Paolo Coppi[q], Elisa Costantini[e], Jelle de Plaa[e], Jan-Willem den Herder[e], Michael DiPirro[b], Chris Done[r], Tadayasu Dotani[a], John Doty[s], Ken Ebisawa[a], Megan Eckart[b], Teruaki Enoto[t], Yuichiro Ezoe[c], Andrew Fabian[p], Carlo Ferrigno[j], Adam Foster[n], Ryuichi Fujimoto[u], Yasushi Fukazawa[v], Akihiro Furuzawa[f], Massimiliano Galeazzi[w], Luigi Gallo[x], Poshak Gandhi[y], Kirk Gilmore[g], Margherita Giustini[e], Andrea Goldwurm[z], Liyi Gu[e], Matteo Guainazzi[a], Daniel Haas[e], Yoshito Haba[aa], Kouichi Hagino[a], Kenji Hamaguchi[b], Atsushi Harayama[a], Ilana Harrus[b], Isamu Hatsukade[ab], Takayuki Hayashi[f], Katsuhiro Hayashi[a], Kiyoshi Hayashida[h], Junko Hiraga[ac], Kazuyuki Hirose[a], Ann Hornschemeier[b], Akio Hoshino[ad], John Hughes[ae], Yuto Ichinohe[c], Ryo Iizuka[a], Yoshiyuki Inoue[a], Hajime Inoue[a], Kazunori Ishibashi[f], Manabu Ishida[a], Kumi Ishikawa[ag], Kosei Ishimura[a], Yoshitaka Ishisaki[c], Masayuki Itoh[ah], Naoko Iwata[a], Naoko Iyomoto[ai], Chris Jewell[aj], Jelle Kaastra[e], Timothy Kallman[b], Tuneyoshi Kamae[g], Erin Kara[i], Jun Kataoka[ak], Satoru Katsuda[al], Junichiro Katsuta[v], Madoka Kawaharada[am], Nobuyuki Kawai[an], Taro Kawano[a], Shigeo Kawasaki[a], Dmitry Khangulyan[ad], Caroline Kilbourne[b], Mark Kimball[b], Ashley King[g], Takao Kitaguchi[v], Shunji Kitamoto[ad], Tetsu Kitayama[ao], Takayoshi Kohmura[ap], Tatsuro Kosaka[aq], Alex Koujelev[ar], Katsuji Koyama[as], Shu Koyama[a], Peter Kretschmar,[aj] Hans Krimm[b], Aya Kubota[at], Hideyo Kunieda[f], Philippe Laurent[z], François Lebrun[z], Shiu-Hang Lee[a], Maurice Leutenegger[b], Olivier Limousin[z], Michael Loewenstein[i], Knox Long[au], David Lumb[aj], Grzegorz Madejski[g], Yoshitomo Maeda[a], Daniel Maier[z], Kazuo Makishima[av], Maxim Markevitch[b], Candace Masters[b], Hironori Matsumoto[aw], Kyoko Matsushita[ax], Dan McCammon[ay], Daniel Mcguinness[b], Brian McNamara[az], Missagh Mehdipour[e], Joseph Miko[b], Jon Miller[ba], Eric Miller[m], Shin Mineshige[t], Kenji Minesugi[a], Ikuyuki Mitsuishi[f], Takuya Miyazawa[f], Tsunefumi Mizuno[v], Koji Mori[ab], Hideyuki Mori[b], Franco Moroso[ar], Harvey Moseley[b], Theodore Muench[b], Koji Mukai[b], Hiroshi Murakami[bb], Toshio Murakami[u], Richard Mushotzky[i], Housei Nagano[f], Ryo Nagino[h], Takao Nakagawa[a], Hiroshi Nakajima[h], Takeshi Nakamori[bc], Toshio Nakano[bd], Shinya Nakashima[a], Kazuhiro Nakazawa[l], Yoshiharu Namba[be], Chikara Natsukari[a], Yusuke Nishioka[ab], Masayoshi Nobukawa[bf], Kumiko Nobukawa[bj], Hirofumi Noda[bg], Masaharu Nomachi[bh], Steve O' Dell[bi], Hirokazu Odaka[a], Hiroyuki Ogawa[a], Mina Ogawa[a], Keiji Ogi[k], Masanori Ohno[v], Masayuki Ohta[a], Takashi Okajima[b], Atsushi Okamoto[am], Tsuyoshi Okazaki[a], Naomi Ota[bj], Masanobu Ozaki[a], Frits Paerels[bk], Stéphane Paltani[j], Arvind Parmar[aj], Robert Petre[b], Ciro Pinto[p], Martin Pohl[j], James Pontius[b], F. Scott Porter[b], Katja Pottschmidt[b], Brian Ramsey[bi], Christopher Reynolds[i], Helen Russell[p], Samar Safi-Harb[bl], Shinya Saito[ad], Shin-ichiro Sakai[a], Kazuhiro Sakai[b], Hiroaki Sameshima[a], Toru Sasaki[ax], Goro Sato[a], Yoichi Sato[am], Kosuke Sato[ax], Rie Sato[a], Makoto Sawada[bm], Norbert Schartel,[aj]

Space Telescopes and Instrumentation 2016: Ultraviolet to Gamma Ray, edited by
Jan-Willem A. den Herder, Tadayuki Takahashi, Marshall Bautz, Proc. of SPIE Vol. 9905, 99050U
 · doi: 10.1117/12.2232379

Peter Serlemitsos[b], Hiromi Seta[c], Yasuko Shibano[a], Maki Shida[a], Megumi Shidatsu[av], Takanobu Shimada[a], Keisuke Shinozaki[am], Peter Shirron[b], Aurora Simionescu[a], Cynthia Simmons[b], Randall Smith[n], Gary Sneiderman[b], Yang Soong[b], Łukasz Stawarz[bn], Yasuharu Sugawara[al], Hiroyuki Sugita[am], Satoshi Sugita[an], Andrew Szymkowiak[q], Hiroyasu Tajima[f], Hiromitsu Takahashi[v], Shin'ichiro Takeda[bo], Yoh Takei[a], Toru Tamagawa[ag], Takayuki Tamura[a], Keisuke Tamura[f], Takaaki Tanaka[as], Yasuo Tanaka[a], Yasuyuki Tanaka[v], Makoto Tashiro[bp], Yuzuru Tawara[f], Yukikatsu Terada[bp], Yuichi Terashima[k], Francesco Tombesi[b], Hiroshi Tomida[a], Yohko Tsuboi[al], Masahiro Tsujimoto[a], Hiroshi Tsunemi[h], Takeshi Tsuru[as], Hiroyuki Uchida[as], Yasunobu Uchiyama[ad], Hideki Uchiyama[bq], Yoshihiro Ueda[t], Shutaro Ueda[a], Shiro Ueno[a], Shin'ichiro Uno[br], Meg Urry[q], Eugenio Ursino[w], Cor de Vries[e], Atsushi Wada[a], Shin Watanabe[a], Tomomi Watanabe[b], Norbert Werner[g], Daniel Wik[af], Dan Wilkins[x], Brian Williams[b], Takahiro Yamada[a], Shinya Yamada[c], Hiroya Yamaguchi[b], Kazutaka Yamaoka[f], Noriko Yamasaki[a], Makoto Yamauchi[ab], Shigeo Yamauchi[bj], Tahir Yaqoob[b], Yoichi Yatsu[an], Daisuke Yonetoku[u], Atsumasa Yoshida[bm], Takayuki Yuasa[ag], Irina Zhuravleva[g], Abderahmen Zoghbi[ba]

[a]Institute of Space and Astronautical Science (ISAS), Japan Aerospace Exploration Agency (JAXA), Kanagawa 252-5210, Japan; [b]NASA/Goddard Space Flight Center, MD 20771, USA; [c]Department of Physics, Tokyo Metropolitan University, Tokyo 192-0397, Japan; [d] Astronomy and Astrophysics Section, Dublin Institute for Advanced Studies, Dublin 2, Ireland; [e]SRON Netherlands Institute for Space Research, Utrecht, The Netherlands; [f] Department of Physics, Nagoya University, Aichi 464-8602, Japan; [g]Kavli Institute for Particle Astrophysics and Cosmology, Stanford University, CA 94305, USA; [h]Department of Earth and Space Science, Osaka University, Osaka 560-0043, Japan; [i]Department of Astronomy, University of Maryland, MD 20742, USA; [j]Department of Astronomy, University of Genova, Versoix CH-1290, Switzerland; [k]Department of Physics, Ehime University, Ehime 790-8577, Japan; [l]Department of Physics, University of Tokyo, Tokyo 113-0033, Japan; [m]Kavli Institute for Astrophysics and Space Research, Massachusetts Institute of Technology, MA 02139, USA; [n]Harvard-Smithsonian Center for Astrophysics, MA 02138, USA; [o]Lawrence Livermore National Laboratory, CA 94550, USA; [p]Institute of Astronomy, Cambridge University, CB3 0HA, UK; [q]Yale Center for Astronomy and Astrophysics, Yale University, CT 06520-8121, USA; [r]Department of Physics, University of Durham, DH1 3LE, UK; [s]Noqsi Aerospace Ltd., CO 80470, USA; [t]Department of Astronomy, Kyoto University, Kyoto 606-8502, Japan; [u]Faculty of Mathematics and Physics, Kanazawa University, Ishikawa 920-1192, Japan; [v]Department of Physical Science, Hiroshima University, Hiroshima 739-8526, Japan; [w]Physics Department, University of Miami, FL 33124, USA; [x]Department of Astronomy and Physics, Saint Mary's University, Nova Scotia B3H 3C3, Canada; [y]Physics & Astronomy, University of Southampton, SO17 1BJ, UK; [z]IRFU/Service d'Astrophysique, CEA Saclay, 91191 Gif-sur-Yvette Cedex, France; [aa]Department of Physics and Astronomy, Aichi University of Education, Aichi 448-8543, Japan; [ab]Department of Applied Physics and Electronic Engineering, University of Miyazaki, Miyazaki 889-2192, Japan; [ac]Department of Physics, School of Science and Technology, Kwansei Gakuin University, 669-1337, Japan; [ad]Department of Physics, Rikkyo University, Tokyo 171-8501, Japan; [ae]Department of Physics and Astronomy, Rutgers University, NJ 08854-8019, USA; [af]Department of Physics and Astronomy, Johns

Hopkins University, MD 21218, USA; [ag]RIKEN Nishina Center, Saitama 351-0198, Japan; [ah]Graduate School of Human Development and Environment, Kobe University, Hyogo 657-8501, Japan; [ai]Kyushu University, Fukuoka 819-0395, Japan; [aj]European Space Agency (ESA), European Space Research and Technology Centre (ESTEC), 2200 AG Noordwijk, The Netherlands; [ak]Research Institute for Science and Engineering, Waseda University, Tokyo 169-8555, Japan; [al]Department of Physics, Chuo University, Tokyo 112-8551, Japan; [am]Tsukuba Space Center (TKSC), Japan Aerospace Exploration Agency (JAXA), Ibaraki 305-8505, Japan; [an]Department of Physics, Tokyo Institute of Technology, Tokyo 152-8551, Japan; [ao]Department of Physics, Toho University, Chiba 274-8510, Japan; [ap]Department of Physics, Tokyo University of Science, Chiba 278-8510, Japan; [aq]School of Systems Engineering, Kochi University of Technology, Kochi 782-8502, Japan; [ar]Space Exploration Development Space Exploration, Canadian Space Agency John H. Chapman Space Centre, QC J3Y 8Y9, Canada; [as]Department of Physics, Kyoto University, Kyoto 606-8502, Japan; [at]Department of Electronic Information Systems, Shibaura Institute of Technology, Saitama 337-8570, Japan; [au]Space Telescope Science Institute, MD 21218, USA; [av]RIKEN, Saitama 351-0198, Japan; [aw]Kobayashi-Masukawa Institute, Nagoya University, Aichi 464-8602, Japan; [ax]Department of Physics, Tokyo University of Science, Tokyo 162-8601, Japan; [ay]Department of Physics, University of Wisconsin, WI 53706, USA; [az]University of Waterloo, Ontario N2L 3G1, Canada; [ba]Department of Astronomy, University of Michigan, MI 48109, USA; [bb]Department of Information Science, Faculty of Liberal Arts, Tohoku Gakuin University, Miyagi 981-3193, Japan; [bc]Department of Physics, Faculty of Science, Yamagata University, Yamagata 990-8560, Japan; [bd]Resarch Center for the Early Universe, University of Tokyo, Tokyo 113-0033, Japan; [be]Department of Mechanical Engineering, Chubu University, Aichi 487-8501, Japan; [bf]Department of Teacher Training and School Education, Nara University of Education, Nara 630-8528, Japan; [bg]Frontier Research Institute for Interdisciplinary Sciences, Tohoku University, Miyagi 980-8578, Japan; [bh] Research Center for Nuclear Physics, Osaka University, Osaka 560-0043, Japan; [bi] NASA/Marshall Space Flight Center, AL 35812, USA; [bj]Department of Physics, Faculty of Science, Nara Women's University, Nara 630-8506, Japan; [bk]Department of Astronomy, Columbia University, NY 10027, USA; [bl]Department of Physics and Astronomy, University of Manitoba, MB R3T 2N2, Canada; [bm]Department of Physics and Mathematics, Aoyama Gakuin University, Kanagawa 252-5258, Japan; [bn]Astronomical Observatory, Jagiellonian University, 30-244, Poland; [bo]Advanced Medical Instrumentation Unit, Okinawa Institute of Science and Technology Graduate University (OIST), Okinawa 904-0495, Japan; [bp] Department of Physics, Saitama University, Saitama 338-8570, Japan; [bq]Science Education, Faculty of Education, Shizuoka University, Shizuoka 422-8529, Japan; [br]Faculty of Health Science, Nihon Fukushi University, Aichi 475-0012, Japan;

ABSTRACT

The *Hitomi* (ASTRO-H) mission is the sixth Japanese X-ray astronomy satellite developed by a large international collaboration, including Japan, USA, Canada, and Europe. The mission aimed to provide the highest energy resolution ever achieved at $E > 2$ keV, using a microcalorimeter instrument, and to cover a wide energy range spanning four decades in energy from soft X-rays to gamma-rays. After a successful launch on 2016 February 17, the spacecraft lost its function on 2016 March 26, but the commissioning phase for about a month provided valuable information on the on-board instruments and the spacecraft

system, including astrophysical results obtained from first light observations. The paper describes the *Hitomi* (ASTRO-H) mission, its capabilities, the initial operation, and the instruments/spacecraft performances confirmed during the commissioning operations for about a month.

Keywords: X-ray, Hard X-ray, Gamma-ray, X-ray Astronomy, Gamma-ray Astronomy, microcalorimeter

1. INTRODUCTION

The *Hitomi* (ASTRO-H) satellite was launched from Tanegashima Space Center of JAXA at 17:45 JST on February 17, 2016. After successfully executing start-up operations, the satellite lost contact with the ground on March 26, with signatures of partial break up of the spacecraft. On April 28, JAXA decided to discontinue the recovery operation of *Hitomi*. This paper reports the mission purpose of *Hitomi* and the technologies achieved through the operations carried out in the commissioning phase.

Our image of the Universe has been dramatically changing from static to dynamic on many scales. X-ray measurements have efficiently detected dynamical and energetic properties of cosmic objects, based on significant improvements in the sensitivity for timing, imaging and spectroscopic studies. High resolution X-ray images, in particular, show dynamical features in the form of shocks, cosmic jets, and outflows of hot gasses. Clusters of galaxies are the largest gravitationally bound objects in the Universe. Many of these systems are now recognized to be undergoing violent mergers characterized by shocks and cold fronts in X-ray and radio images. Supermassive black holes are found in many galaxies, surrounded by a dense gas in some cases, and their co-evolution with the host galaxies over the cosmological timescale is an important issue still to be understood. Breakthroughs in X-ray observation techniques would bring us new views about the evolution of these objects.

High resolution spectroscopy combined with a wide-band energy coverage is a very powerful way of looking into the dynamical evolution of the Universe through X-ray observations. Energy resolution as high as $\Delta E < 7$ eV would enable us to measure Doppler motions with an accuracy of ~ 100 km s^{-1} at 6 keV. Sensitivity up to 600 keV, combined with imaging capability up to 80 keV, will show us the highest energy regions and the spatial distribution of the accelerated particles. Our current knowledge on how much and in what form the non-thermal energy is produced and carried in each system is still quite poor. The great advance in the energy resolution and wide-band coverage of *Hitomi* marked us a substantial advance in probing all forms of energy in cosmic objects. Such an improvement in X-ray astronomy is thought to match well with the recent progress ocurring in radio and gamma-ray bands.

The *Hitomi* (ASTRO-H) mission has been designed to achieve these aims.[1–8] This is an international X-ray satellite which was launched with the 30th H-IIA rocket. NASA selected US participation on ASTRO-H as a Mission of Opportunity in the Explorer Program category. Under this program, the NASA/Goddard Space Flight Center collaborates with ISAS/JAXA on the implementation of the X-ray microcalorimeter and the soft X-ray telescopes (SXS Proposal NASA/GSFC, 2007). Other institutional members of the collaboration are SRON*, Geneva University, CEA/IRFU†, CSA‡, Stanford University, and ESA. In early 2009, NASA, ESA and JAXA selected thirteen science advisors to provide scientific guidance to the ASTRO-H project. The ESA contribution to the ASTRO-H mission includes the procurement of payload hardware elements that enhance the scientific capability of the mission.

In this paper, we describe the *Hitomi* (ASTRO-H) satellite and the on-board instruments, along with the in-orbit performances of some of the satellite systems.

2. SPACECRAFT

There are four focusing telescopes mounted on the top of a fixed optical bench (FOB). Two of the four telescopes are Soft X-ray Telescopes (SXTs) and they have a 5.6 m focal length. They focus soft-energy

*Netherlands Institute for Space Research

†French Alternative Energies and Atomic Energy Commission (CEA)/Institute of Research into the Fundamental Laws of the Universe (IRFU)

‡Canadian Space Agency

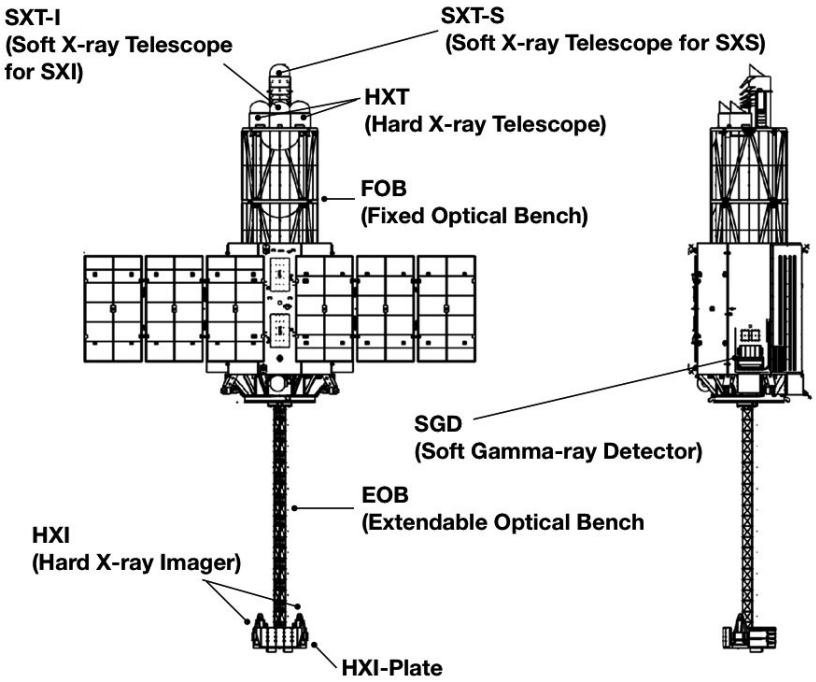

Figure 1. Schematic view of the *Hitomi* satellite with the Extendable Optical Bench deployed. The total length of the satellite is about 14 m.[8,10–12]

Figure 2. A photograph of the *Hitomi* Satellite.

Table 1. Key parameters of the payload

Parameter	Hard X-ray Imager (HXI)	Soft X-ray Spectrometer (SXS)	Soft X-ray Imager (SXI)	Soft γ-ray Detector (SGD)
Detector technology	Si/CdTe cross-strips	micro calorimeter	X-ray CCD	Si/CdTe Compton Camera
Focal length	12 m	5.6 m	5.6 m	–
Effective area	300 cm^2 @ 30 keV	300 cm^2 @6 keV 250 cm^2 @1 keV	350 cm^2 @6 keV 370 cm^2 @1 keV	>20 cm^2@100 keV Compton Mode
Energy range	5 –80 keV	0.3 – 12 keV	0.4 – 12 keV	60 – 600 keV
Energy resolution (FWHM)	< 2 keV (@60 keV)	< 7 eV (@6 keV)	< 200 eV (@6 keV)	< 4 keV (@60 keV)
Angular resolution	1.9 arcmin (@30 keV)	∼1.2 arcmin	∼1.3 arcmin	–
Effective Field of View	$\sim 9 \times 9$ $arcmin^2$	$\sim 3 \times 3$ $arcmin^2$	$\sim 38 \times 38$ $arcmin^2$	0.6×0.6 deg^2 (< 150 keV)
Time resolution	25.6 μs	5 μs	4 sec/0.1 sec	25.6 μs
Operating temperature	-20°C	50 mK	-120°C	-20°C

X-rays (E $\sim$ 0.3–12 keV) onto focal plane detectors mounted on the base plate of the spacecraft (see Fig. 2). One SXT points to a microcalorimeter spectrometer array in the Soft X-ray Spectrometer (SXS) with excellent energy resolution of <7 eV, and the other SXT points to a large-area CCD array in the Soft X-ray Imager (SXI). The other two telescopes are Hard X-ray Telescopes (HXTs) capable of focusing high-energy X-rays (E = 5–80 keV). The focal length of the HXTs is 12 m. The Hard X-ray Imager (HXI) consists of two detector units which are mounted on the HXI plate, at the end of a 6 m extendable optical bench (EOB) that is stowed to fit in the launch fairing and deployed once in orbit. In order to extend the energy coverage to the soft γ-ray region up to 600 keV, the Soft Gamma-ray Detector (SGD) was implemented as a non-focusing detector. Two SGD detectors, each consisting of three units are mounted separately on two sides of the satellite. With these instruments, *Hitomi* covered the entire bandpass between 0.3 keV and 600 keV. The key parameters of those instruments are summarized in Table. 1.

The lightweight design of the EOB renders it potentially vulnerable to distortions from thermal fluctuations in low-Earth orbit (LEO) and spacecraft attitude maneuvers. Over the long exposures associated with X-ray observing, such fluctuations might impair HXI image quality unless a compensation technique is employed. To provide the required corrections, the Canadian contribution is a laser metrology system (the Canadian ASTRO-H Metrology System, CAMS) aiming at measuring displacements in the alignment of the HXT optical path. Two laser and detector modules (CAMS-LD-1 and -2) located on the top plate of the FOB, and two passive target modules (CAMS-T-1 and -2), each consisting of a retroreflector (corner cube mirror) mounted on the EOB detector plate (HXI plate).[16]

Almost all of onboard subsystems, such as the command/data handling system, the attitude control system, and four types of X-ray/gamma-ray telescope instruments, are connected to the SpaceWire network using a highly redundant topology.[17] The number of physical SpaceWire links between components exceeds 140 connecting ∼40 separated components (i.e., separated boxes), and there are more links in intra-component (intra-board) networks. Most of the electronics boxes of both the spacecraft bus and the scientific instruments are mounted on the side panels of the spacecraft. The electronics boxes for the HXI are mounted on the HXI plate.

3. ON-ORBIT OPERATION

ASTRO-H was launched with the 30th H-IIA rocket at 17:45 JST on February 17, and injected into an approximately circular orbit with an altitude of 575 km and an inclination of 31 degrees (Table 2). The

Table 2. *Hitomi* Mission

Launch site	Tanegashima Space Center, Japan
Launch vehicle	JAXA H-IIA rocket
Orbit Altitude (Apogee)	576.5 km
Orbit Altitude (Perigee)	574.4 km
Orbit Type	Approximate circular orbit
Orbit Inclination	31 degrees
Total Length	14 m
Mass	2.7 metric ton
Power	< 3500 W

launch operation went smoothly, and the orbit was exactly as planned. ASTRO-H was named *Hitomi*, which means pupil in Japanese, and it was hoped that the observatory will function as a powerful eye to look into the X-ray emitting processes operating in a wide range of objects. As mentioned before, the *Hitomi* satellite lost contact with the ground on March 26. The reports on the analysis of the cause of the anomalous events are given on the JAXA homepage: `http://global.jaxa.jp/projects/sat/astro_h/topics.html`.

After initial operations of the spacecraft, including the tuning of the attitude control system and the start-up of the SXS coolers, we commenced operation of the EOB at the end of which the HXI plate was mounted. On February 27th, we turned on the electronics of the EOB (EOB-E). On the same day, a laser of the CAMS-LD was turned on, in order to monitor the orientation of the EOB during its deployment. On the next day, we carried out operation of the EOB deployment. Since the HXI plate was quite heavy, ~ 150 kg in total, a lateral shake developed by degrees as the EOB mast was being extended. This is because the mast is not stiff enough during deployment to sustain the heavy HXI plate since the mast is composed of multiple joints and hence has some mechanical looseness. Accordingly, lateral angular velocity sometimes approached a software limit, so we carried out the deployment intermittently. We achieved the final full extension configuration of the EOB using four contact passes.

In Fig. 3 (left), we show the time history of the center position of the EOB (EOB-X and EOB-Y), its rotation around the spacecraft Z axis from the nominal orientation, and an apparent unbiased distance (EOB-r12p) throughout *Hitomi*'s life from the start of the EOB extension. EOB-r12p is a difference between measured and actual distance between two corner cubes. The value of 0.5 mm or less indicates that the CAMS system was well calibrated and aligned as a whole.

The times of maneuvers are drawn with the vertical lines. The time of the EOB extension is clearly marked by a jump of the center positions of the HXI plate measured by CAMS. After that, however, the location of the HXI plate is mostly within 0.5 mm in peak-to-bottom (note that 1 arcsec at a distance of 12 m is 0.0582 mm). Within a single observation (during time interval of two adjacent maneuvers), jitter of the HXI plate is as small as ~ 0.2 mm. This is comparable or smaller than the pixel size of the HXI detector. The stability of the image at the focal plane was monitored with CAMS. As shown in Fig. 3 (right) , the movement of the focal plane image is less than 400 μm corresponding to about 7 arcsec. We conclude that we achieved a highly stable EOB.

The microcalorimeter array of SXS has a linear size of 5 mm and is located at the focal plane of the telescope SXT-S. This gives the angular size covered by SXS to be 3.1 arcmin. Also, the HXT, with focal length 12 m, has a vignetting angle of 1 arcmin. Therefore, the mutual alignment to enable both SXS and HXI to observe an object right at the optical axes of the telescopes took a lot of effort. As a result, the pointing of an object at the center of the SXS instrument gave images right at the expected positions for the SXI, HXI-1 and HXI-2 instruments.

Since *Hitomi* was in a low-earth orbit, with the attitude pointed to a direction in the inertial frame, the satellite conditions change throughout one orbit. The temperature gradient changes depending on the day and night phases, and the albedo from the earth, also gravity gradient on the spacecraft change largely in the orbit. In order to fulfill the requirement of the pointing control accuracy of $\sim$60 arcsec, the thermal

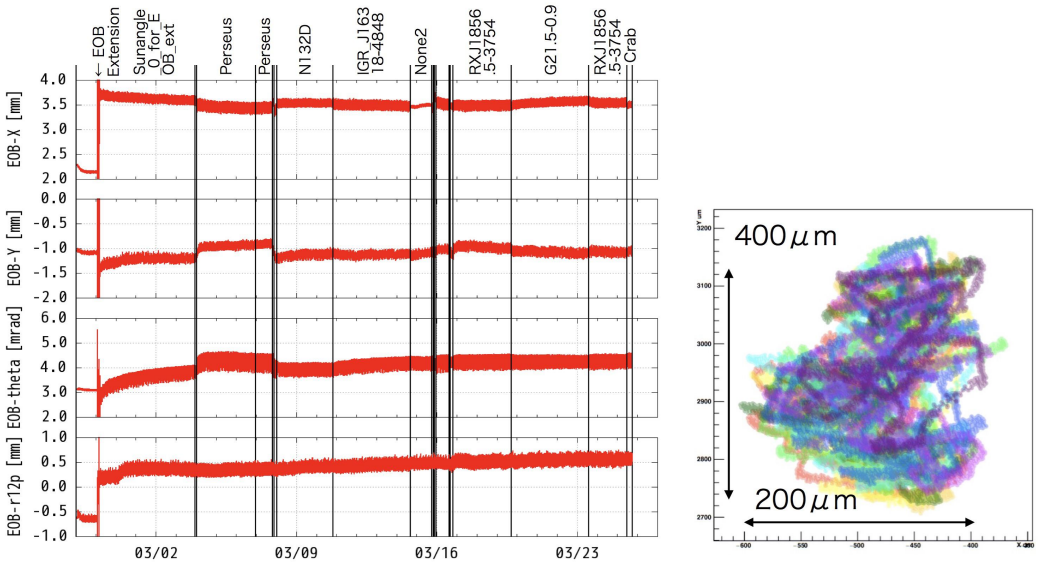

Figure 3. (left) The time history of the center position of the EOB (EOB-X and EOB-Y), its rotation around the spacecraft Z axis from the nominal orientation, and an apparent unbiased distance between the two corner cubes. (right) Stability of the focal plane alignment measured in about a day with CAMS after the EOB extension.

design needs to be very precise. The temperatures measured by HCE (Heater Control Electronics) sensors at various spacecraft positions were all within the acceptable range. Also, temperature data after the start-up of mission instruments, after March 20, were mostly within 5°C of the predicted values.[13] There are differences of 7°C in some instruments, but no data show deviations larger than 10°C. During extending the EOB, the temperature of the HXI plate, after the switch off of HXI-HCE, dropped by about 16°C as expected from the thermal analysis.

Along with the parameter tuning operation for the satellite bus and the attitude system, we observed several X-ray sources. The main purpose of the observations was the calibration of X-ray instruments, but the sources also provided interesting scientific data. The observed sources are the Perseus cluster (February 25–27, March 4–8), N132D (March 8–11), IGR J16318-4848 (March 11–15), RXJ 1856-3754 (March 17–19, 23–25), G21.5-0.9 (March 19–23), and the Crab Nebula (March 25). The SXS was operational before the Perseus cluster observation, and SXI started observation during the pointing to Perseus. The HXI1 and HXI2 were started in March 8–15, and SGD in March 16–25. All the instruments finished their start-up operations on the day before the loss of contact. The *Hitomi* data will be archived in the public archive at the DARTS (JAXA/ISAS) and HEASARC (NASA/GSFC) after one year propriety period that starts when the final data processing is completed.[14]

The first light observation of the Perseus cluster unequivocally showed the superb spectroscopic performance of the SXS by revealing the narrow line complex of He-like ion of iron around 6.7 keV from the core of the Perseus Cluster.[15]

4. SCIENCE INSTRUMENTS

Instruments onboard the *Hitomi* Satellite include a high-resolution, high-throughput spectrometer (SXS) sensitive over 0.3–12 keV with high spectral resolution of $\Delta E < 7$ eV, enabled by a microcalorimeter array located in the focal plane of thin-foil X-ray optics; hard X-ray imaging spectrometers (HXI) covering 5–80 keV, located in the focal plane of multilayer-coated, focusing hard X-ray mirrors; a wide-field imaging spectrometer sensitive over 0.4–12 keV, with an X-ray CCD camera (SXI) in the focal plane of a soft X-ray telescope; and a non-focusing Compton-camera type soft gamma-ray detector (SGD), sensitive in the 60–600 keV band.

Figure 4. Photographs of flight models of (left) Soft X-ray telescope, SXT-S and (right) hard X-ray telescope, HXT-1.

In the following sections, these instruments are briefly described. Detailed descriptions of the instruments and their current status are available in other papers.

4.1 Soft X-ray Telescopes

The X-ray mirror is very similar to the *Suzaku* X-ray Telescope,[20] but with a longer focal length of 5.6 m and a larger outer diameter of 45 cm. The SXT[21–25] consists of three parts: an X-ray mirror, a stray light baffle called the pre-Collimator, and a thermal shield to keep the mirror temperature at around 20°C. The mirror is a conically approximated Wolter I grazing incidence optic with 203 nested shells. Each shell is segmented into four quadrants.

The flight SXT mirror assemblies (Fig. 4 left), SXT-I for the SXI and SXT-S for the SXS, were fabricated at NASA/GSFC and delivered to JAXA. According to calibration at GSFC and ISAS, the angular resolution (Half Power Diameter : HPD) is 1.3 arcmin and 1.2 arcmin for the SXT-I and SXT-S, respectively. The result obtained with SXT-S exceeds the desired goal. Effective areas were measured to be $\sim$590 cm^2 at 1 keV and $\sim$430 cm^2 at 6 keV. The system net effective area at 1 and 6 keV is about 250 and 300 cm^2 for the SXS, and 370 and 350 cm^2 for the SXI, respectively. However, since the SXS gate valve (GV) was closed during observations, the SXS effective area was reduced by the Be window transmission and the GV obscuration. The SXS net effective area with the GV closed was about 160 cm^2 at 6 keV with almost no area below 2 keV.

According to the in-flight data, the SXT-I and SXT-S were clearly focusing X-rays onto the corresponding detectors and they seemed to be working as expected. The overall effective area (flux) was examined using the Crab and the G21.5-0.9 data. Model fittings for both spectra produced a power-law photon index consistent with the previous measurements[18,19] which indicates that the effective area response was consistent with the ground calibration results. As far as we have so far been able to deduce from the limited amount of data, the SXT worked properly. A more detailed examination is our future task.

4.2 Hard X-ray Telescopes

A depth-graded multi-layer mirror reflects X-rays not only by total external reflection but also by Bragg reflection. In order to obtain a high reflectivity up to 80 keV, the HXT consists of a stack of multilayers with different sets of periodic length and number of layer pairs with a platinum/carbon coating. The technology of a hard X-ray focusing mirror has already been proven by the balloon programs InFOCμS (2001, 2004),[26,27] HEFT (2004)[28] and SUMIT (2006)[26] and recently with the NuSTAR satellite.[29]

The HXT[30–35] consists of three parts, an X-ray mirror: a stray light baffle called pre-Collimator, and a thermal shield (Fig. 4, right). The mirror is based on conically-approximated Wolter I grazing incidence optics.[32,33] The diameters of the innermost and the outermost reflectors are 120 mm and 450 mm, respectively. The total number of nested shells is 213. Since a telescope module is made up from three segments with an azimuthal opening angle of 120° each, it requires 1278 reflectors in total. Production of two flight-ready HXT mirror assemblies, HXT-1 and HXT-2, was completed in 2014. According to calibration performed by using the SPring-8 beam line, the characteristics of HXT-1 and HXT-2 are quite similar. Based on ground calibration at the synchrotron radiation facility SPring-8, a collecting area of 174 cm^2 at 30 keV for one telescope has been achieved, resulting in a total effective area of 348 cm^2. The half power diameter of the HXTs is $\sim$1.9 arcmin at 30 keV.[35]

After the launch, the first light data were obtained from an observation of the supernova remnant G21.5-0.9. The HPD of the two HXT modules was both 1.8 arcmin in the band 20-30 keV, which seems better than that obtained from the ground calibration by 0.1 arcmin. Note, however, that the encircled energy fraction was normalized at $r = 6$ arcmin on the ground whereas, due to the limitation of the HXI field of view, it is made at $r = 4$ arcmin inflight and the data in the area $r > 4$ arcmin are subtracted as background. We therefore reprocessed the ground calibration data in the same way as the in-flight data. As a result, we found that the encircled energy fractions on ground and inflight coincide within $\sim$5% in the area $r > 1$ arcmin. We have also analyzed the spectrum of G21.5$-$0.9. Using a broken power-law mode with all parameters but a normalization being equal to NuSTAR's,[36] we obtained a flux of 5.09 ± 0.06 erg cm^{-2} s^{-1} in the 15$-$50 keV, which agrees with that obtained by NuSTAR within 0.5%.

4.3 Soft X-ray Spectrometer System

The soft X-ray spectrometer system consists of the Soft X-ray Telescope (SXT), the Filter Wheel (FW) assembly,[37] and the SXS.[38–41] The SXS is a 36-pixel system with an energy resolution of better than 7 eV between 0.3–12 keV. The array design for the SXS is basically the same as that for the *Suzaku*/XRS,[42] but has larger pixel pitch and absorber size. HgTe absorbers are attached to ion-implanted Si thermistors formed on suspended Si micro-beams.[43–45] The 6×6 array of silicon thermistors on an 832 μm pitch was manufactured during the *Suzaku*/XRS program along with arrays with smaller pitch as an option for a larger field of view (Fig. 5 (left)). For SXS, improved heat-sinking was added to the frame of the array, and HgTe absorbers with very low specific heat were attached to the pixels. The width of the individual absorbers was 819μm.[45] The sensor was installed in the Dewar (Fig. 5 (right))

The SXS cooling system must cool the array to 50 mK with sufficient duty cycle to fulfill the SXS scientific objectives: this requires extremely low heat loads. To achieve the necessary gain stability and energy resolution, the cooling system must regulate the detector temperature at 50 mK, to within 2 μK rms over intervals of about half an hour, for at least 24 hours per cycle.[47] From the detector stage to room temperature, the cooling chain is composed of a 3-stage Adiabatic Demagnetization Refrigerator (ADR),[46] superfluid liquid ^{4}He (hereafter LHe), a ^{4}He Joule-Thomson (JT) cryocooler, and two-stage Stirling cryocoolers.

In order to obtain a good performance for bright sources, a filter wheel (FW) assembly, which includes a wheel with selectable filters and a set of modulated X-ray sources, were provided by SRON and Univ. of Geneva. This was placed at a distance of 90 cm from the detector. The FW is able to rotate a suitable filter into the beam to optimize the quality of the data, depending on the source characteristics.[37] In addition to the filters, a set of on-off-switchable X-ray calibration sources, using a light sensitive photo-cathode, were available. With these calibration sources, the energy scale could be calibrated with a typical 1$-$2 eV accuracy, allowing proper gain and linearity calibration of the detector in flight.

All SXS components except for the SXS power distributor (SXS-DIST) were cold-launch (no power at launch). The first critical operation was to reestablish the He plumbing in space.[50] Quickly after the fairing opened, the He vent valve was opened, which was confirmed by the telemetry during the first contact 50 minutes after the launch. We next focused on starting the cooling chain. On day 0, we started two shield coolers (SC) at the full wattage, and two pre-coolers (PC) at a low wattage. On day 1, the PCs were also ramped up to the full wattage. By day 4, the Joule-Thomson cooler (JTC) was also ramped up step by step. On day 5, the ADR cool down was started and the sensor was cooled to 50 mK. After that, the cooling

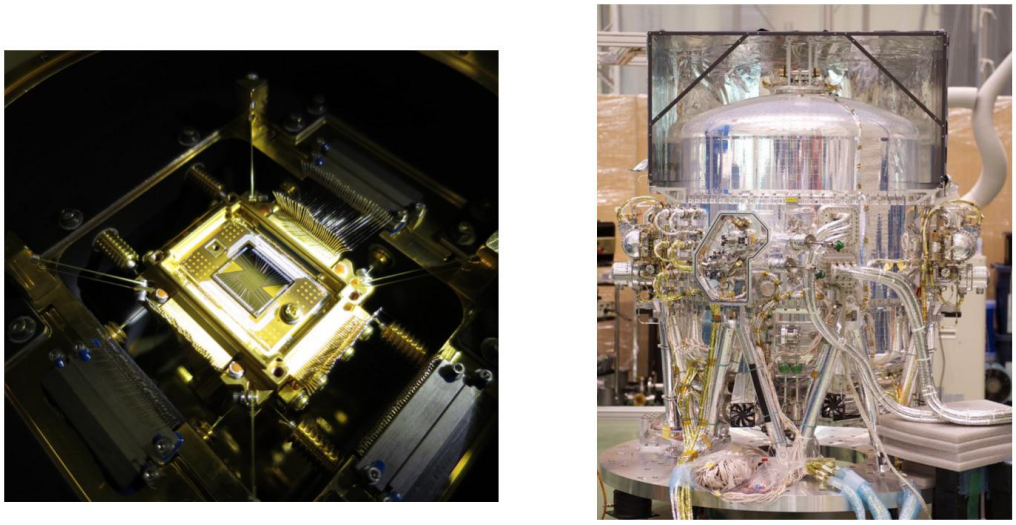

Figure 5. Photographs of (left) SXS sensor and (right) SXS Dewar. The sensor was suspended from the outer structure using Kevlar, and electrical connections to the housing were made using tensioned wires to reduce the sensitivity to microphonics.The outer shell of the Dewar is 950 mm in diameter.

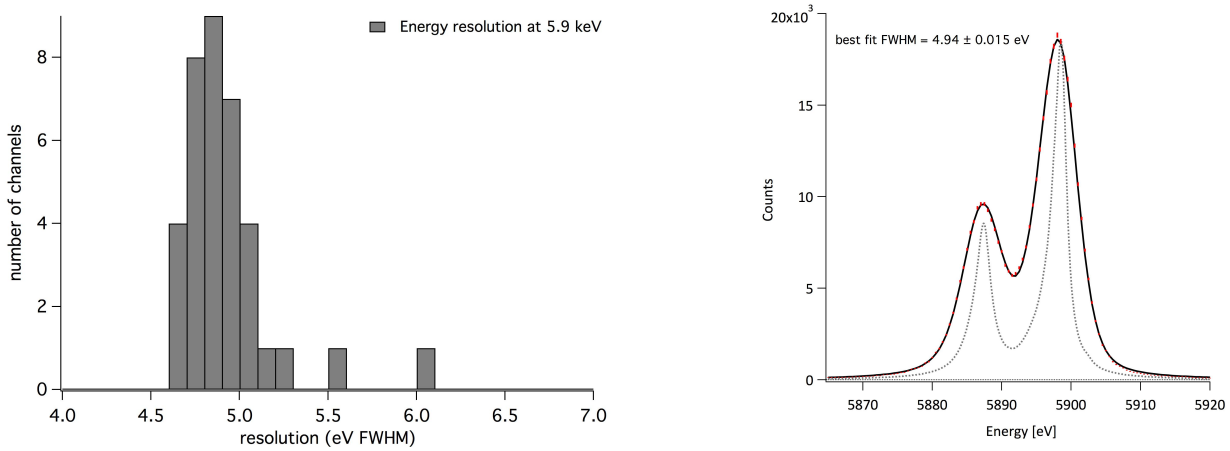

Figure 6. (left) A histogram of the distribution of resolutions measured across the array. (right) the whole-array spectrum around 5.9 keV. The points are the data, with sqrt(N) error bars on the counts barely visible. The dark line is the best fit to a model of the natural line shape convolved with Gaussian broadening, and the dashed gray line is the natural line shape.

chain worked without any problem until the end of the mission by repeating ADR recycles periodically and continuously operating the cryo-coolers.

The signal chain was also started within the first week. On day 2, both the analogue and digital signal processors were started (respectively called XBOX and PSP). After the initial check and the parameter setting, the first noise measurement was performed on day 2 at a warm detector temperature and on day 5 at the 50 mK temperature.

The SXS was ready for observations by as early as day 6. On day 7, the spacecraft was pointed to the Perseus cluster, and we observed X-rays from an astronomical target for the first time. Although the pointing was offset from the cluster core by a few arc minutes, we obtained sufficient counts to make an offset correction based on our own count rate map within a few cycles. On day 8, an adjustment maneuver was made toward the core of the cluster for a longer exposure time.

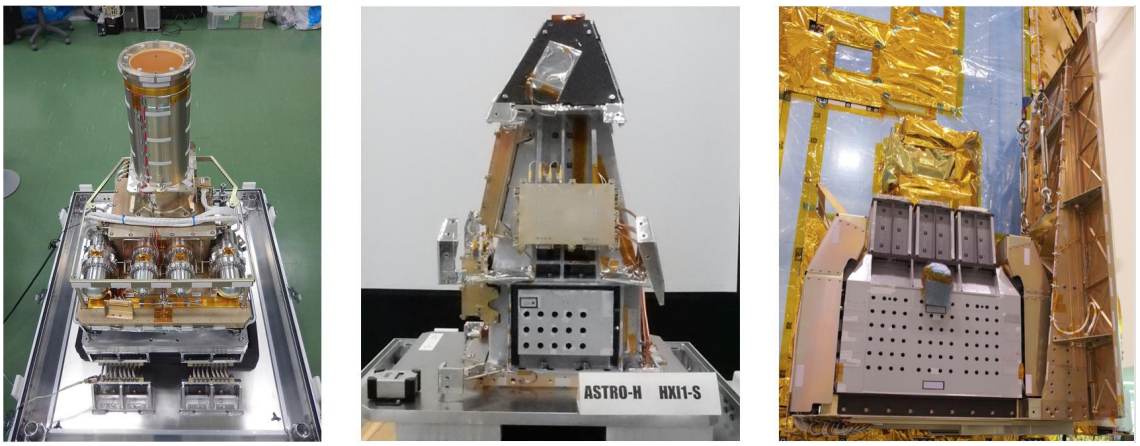

Figure 7. Photographs of SXI (left), HXI (center), and SGD (right)

After the EOB extension, we started commissioning the filter wheel electronics (FWE), which was the last SXS subsystem to be powered. The filter wheel was rotated on day 30 in order to provide X-ray illumination of the whole array by ^{55}Fe sources. The resulting calibration data set was used to refine the gain scales and measure the energy resolutions of the individual pixels. Fig. 6 (left) is a histogram of the distribution of resolutions measured across the array. The composite resolution of the whole array was 4.9 eV (Fig. 6 (right)).[45,48,49]

What remained to be done during the commissioning phase but was not completed were: (i) the start up of the modulated X-ray source, (ii) opening of the gate valve, and the start of the temperature control of the Dewar main shell filter, and (iii) the final setting of the event threshold. The cryogen-free operation using the third stage ADR, which was planned in later phase of the mission,[51] was also not carried out.

4.4 Soft X-ray Imager

X-ray sensitive silicon charge-coupled devices (CCDs) are key detectors for X-ray astronomy. The low background and high energy resolution achieved with the XIS/*Suzaku* clearly show that the X-ray CCD can also play a very important role in the mission. The soft X-ray imaging system is consisted of an imaging mirror, the Soft X-ray Telescope (SXT-I), and a CCD camera, the Soft X-ray Imager (SXI), as well as the cooling system.[52–57] Fig. 7 (left) shows a photograph of the SXI detector. The SXI camera contains a cold plate on which four CCDs are placed. The cold plate is connected to two identical Stirling coolers.

Start-up operation of SXI began from March 2, 2016. The nominal operation temperature of -110°C was reached on March 7, and we started data acquisition in the event mode. A single-stage Stirling cooler was used to cool down the CCDs. Fine control of temperature was performed with heaters, and we confirmed the temperature stability same as that during the ground tests. We employed a charge injection technique from the beginning of the operation to cope with the decrease of the charge transfer efficiency due to the radiation damage. Artificial charge was injected from the top of columns of the CCDs at every 160 rows (before the on-chip 2x2 binning). We confirmed that the noise level of CCDs was about 5$-$7 e$^-$ rms, the same as that of the ground tests. We also confirmed that the amount of the injected charge was not changed from the ground test.

The first target was the Perseus cluster of galaxies. As shown in Fig. 8 (left), the cluster image is offset from the SXI center, because the CCDs were placed to have an offset relative to the aim point of SXT-I by 5 arcmin to avoid the CCD gaps. Two calibration sources of ^{55}Fe are also seen as semicircular images on top and bottom centers. Initial performance of SXI was checked using these calibration source data and the Perseus data. The gain and the energy resolution of the CCDs were found to be consistent with the ground data. Thus we confirmed that SXI functioned properly on orbit. We accumulated background data from the non source regions of the SXI field of view. In the case of *Suzaku* XIS(BI),[58] non-X-ray background (NXBG) increased rapidly above 6 keV. Such an increase of NXBG almost disappeared in SXI thanks to the

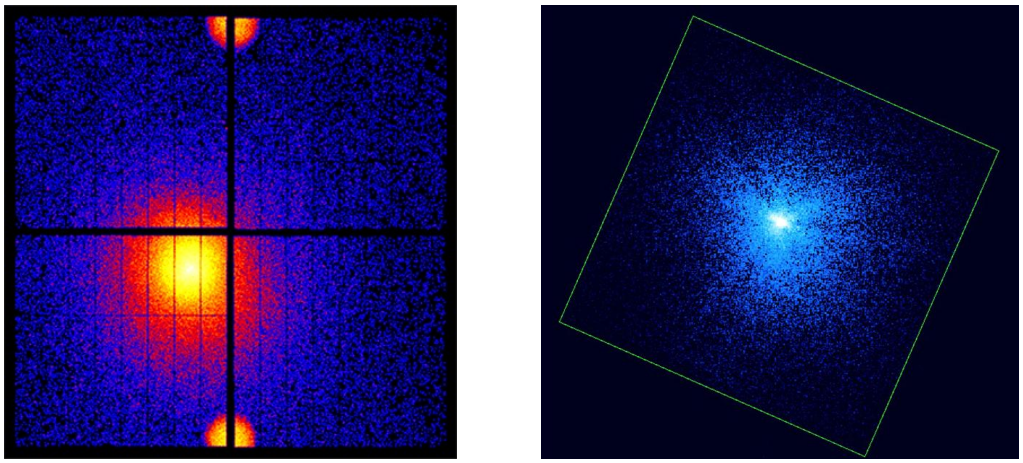

Figure 8. (left) A logarithmically scaled image of the Perseus cluster. Its core is just on the aim point of the SXI. Two calibration areas are seen as bright regions on top and bottom center. The size of the image is 38×38 arcmin^2.[57] (right) A logarithmically scaled image of the Crab Pulsar for 10-50 keV energy band, extracted from the HXI-1 data of the Crab observation. The square in the image corresponds to the 9.1×9.1 arcmin^2 FOV of the HXI. Note that the correction of the satellite attitude is preliminary and vignetting correction is not yet applied.[66]

thick depletion layer (200 μm) compared to that of XIS(BI) ($\sim$42 μm). Furthermore, Ni lines in the NXB spectrum became much weaker, while the Au lines became more prominent.

4.5 Hard X-ray Imager (HXI)

There are two HXI sensor modules, HXI1-S and HXI2-S (Fig. 7 (center)). The sensor part of the HXI[59–66] consisted of four layers of 0.5 mm thick Double-sided Silicon Strip Detectors (DSSD) and one layer of 0.75 mm thick CdTe imaging detector. In this configuration, soft X-ray photons below $\sim$ 20 keV are absorbed in the Si part (DSSD), while hard X-ray photons above $\sim$ 20 keV go through the Si part and are detected by a newly developed CdTe double-sided cross-strip detector. In order to reduce the background、 the sensor part is surrounded by a thick active shield and collimator made of BGO scintillator coupled to avalanche photo diodes (APDs). In addition to the increase in efficiency, the stack configuration and individual readouts provide information on the interaction depth. This depth information is very useful to reduce the background in space applications, because we can expect that low energy X-rays interact in the upper layers and, therefore, it is possible to reject the low energy events detected in lower layers. The $E < 20$ keV spectrum, obtained with the DSSD Si detector, has a much lower background due to the absence of activation in heavy material, such as Cd and Te. The DSSDs cover the energy below 30 keV while the CdTe strip detector covers the 20–80 keV band.

The electronics boxes of the HXIs (HXI-DE, DPU and AE) were powered on 28-29 February. Then, the HXI sensor (HXI-S) parts temperature were gradually decreased from 5 °C to -25 °C followed by the bias voltage operation of HXI1-S on 8 March. The APD bias, Si imager bias and CdTe imager bias were raised to their operational voltage step-by-step, and the HXI1-S became operational on 12 March. The HXI2-S followed on 15 March. All 1280 read-out channels for each of the HXI1-S and HXI2-S camera performed well, showing noise performance consistent with the pre-launch on-ground measurements. An image of the Crab Pulsar taken with the HXI-1 is shown in Fig. 8 (right).[66]

In addition to the thick BGO active shield and the concept of multi-layer configuration of the imager, CXB baffling within the detector and inside the spacecraft worked well to reduce the background. The HXI achieved a low background level of 1–1.3×10^{-4} cnt s^{-1} cm^{-2} at 20–30 keV (here, the flux is normalized by the geometrical size of the detector, 10 cm^2), which is the lowest level ever achieved in orbit. Thanks to the optimum design of the HXT and the long focal length of 12 m, the effective area was also the largest among the hard X-ray imaging spectroscopy instruments, flown to date. The HXI showed the potential to provide the highest sensitivity in this energy band, especially for diffuse sources.

4.6 Soft Gamma-ray Detector (SGD)

The SGD[69–74] measures soft γ-rays via reconstruction of Compton scattering in the Compton camera, covering an energy range of $40 - 600$ keV with a sensitivity at 300 keV, 10 times better than that of the *Suzaku* Hard Xray Detector, by adopting a new concept of a narrow-FOV (Field of View) Compton telescope, combining Compton cameras and active well-type shields. There are two SGD sensor modules, SGD1 and SGD2. In the Si/CdTe Compton camera, events involving the incident gamma-ray being scattered in the Si detector and fully absorbed in the CdTe detectors are used for Compton imaging. The direction of the gamma-ray is calculated by solving the Compton kinematics with information concerning deposit energies and interaction positions recorded in the detectors. In principle, each layer could act not only as a scattering part but also as an absorber part. A very compact, high-angular resolution (fineness of image) camera is realized by fabricating semiconductor imaging elements made of Si and CdTe, which have excellent performance in position resolution, high-energy resolution, and high-temporal resolution. The detector consists of 32 layers of 0.6 mm thick Si pad detectors and eight layers of CdTe pixellated detectors with a thickness of 0.75 mm. The sides are also surrounded by two layers of CdTe pixel detectors.

The camera was then mounted inside the bottom of a well-type active shield. The major advantage of employing a narrow FOV is that the direction of incident γ-rays is constrained to be inside the FOV. If the Compton cone, which corresponds to the direction of incident gamma-rays, does not intercept the FOV, we can reject the event as background. Most of the background can be rejected by requiring this condition. The opening angle provided by the BGO shield is $\sim$10 degrees at 500 keV. An additional PCuSn collimator restricts the field of view of the telescope to $30'$ for photons below 100 keV, to minimize the flux due to the cosmic X-ray background in the FOV. Fig. 7 (right) shows a photograph of the SGD detector module.

The Power-on operation of SGD-DE, SGD-DPU and SGD-AE was performed on March 1 2016.[74] After this operation, SGD HK telemetries including temperature monitors of SGD-S were generated. Then, the SGD-S was gradually cooled down to $-25°$C from March 3 to March 13 by changing the SGD heater settings. Start-up operation of SGD-S began on March 15, 2016. First, Compton cameras, APD-CSA and HV modules for Compton cameras and APDs were powered on, and then we applied the high voltage step by step basis and set up detectors into the nominal observation mode. From March 21, SGD1-S had been operated in the nominal observation mode, and SGD2-S was shifted into the nominal observation on March 24 2016.

5. SUMMARY

Carrying onboard the two types of X-ray optics and the four types of detectors, ASTRO-H (*Hitomi*) was designed to provide exciting wide-band and high-energy-resolution data on various high-energy astrophysical objects. Its one month of operation in orbit demonstrated that many of the new technologies introduced to the *Hitomi* mission worked well. In fact, all instruments produced data with satisfactory quality, though for a short period, until the loss of spacecraft capability. In particular, the acquired data clearly verified the key properties of the SXS, i.e., the high spectral resolution ($\sim$5 eV FWHM) for both point and diffuse sources over a broad $0.3-12$ keV bandpass, with the low non-X-ray background ($<1.0\times10^{-3}$ cts s^{-1}keV^{-1}). Although the gate valve was not opened, the effective area was consistent with the designed value, indicating that an effective area of 250 cm^2 at 1 keV and 300 cm^2 at 6 keV would be achieved if the GV was open. *Hitomi* has thus opened the door to a new generation of X-ray astronomy; forthcoming scientific papers based on the limited amount of data will clearly show the power of this challenging mission.

Acknowledgments

We acknowledge all the JAXA members who have contributed to the ASTRO-H (*Hitomi*) project. All U.S. members gratefully acknowledge support through the NASA Science Mission Directorate. Stanford and SLAC members acknowledge support via DoE contract to SLAC National Accelerator Laboratory DE-AC3-76SF00515 and NASA grant NNX15AM19G. Part of this work was performed under the auspices of the U.S. DoE by LLNL under Contract DE-AC52-07NA27344 and also supported by NASA grants to LLNL. Support from the European Space Agency is gratefully acknowledged. French members acknowledge support from CNES, the Centre National d'Etudes Spatiales. SRON is supported by NWO, the Netherlands Organization

for Scientific Research. Swiss team acknowledges support of the Swiss Secretariat for Education, Research and Innovation SERI and ESA's PRODEX programme. The Canadian Space Agency is acknowledged for the support of Canadian members. We acknowledge support from JSPS/MEXT KAKENHI grant numbers 15H02070, 15K05107, 23340071, 26109506, 24103002, 25400236, 25800119, 25400237, 25287042, 24540229, 25105516, 23540280, 25400235, 25247028, 26800095, 25400231, 25247028, 26220703, 24105007, 23340055, 15H00773, 23000004 15H02090, 15K17610, 15H05438, 15H00785, and 24540232. H. Akamatsu acknowledges support of NWO via Veni grant. M. Axelsson acknowledges JSPS International Research Fellowship. C. Done acknowledges STFC funding under grant ST/L00075X/1. P. Gandhi acknowledges JAXA International Top Young Fellowship and UK Science and Technology Funding Council (STFC) grant ST/J003697/2. H. Russell acknowledges support from ERC Advanced Grant Feedback 340442. We thank contributions by many companies, including in particular, NEC, Mitsubishi Heavy Industries, Sumitomo Heavy Industries, and Japan Aviation Electronics Industry. We thank the support from the JSPS Core-to-Core Program.

REFERENCES

[1] NeXT Satellite Proposal,the NeXT working group, submitted to ISAS/JAXA (2003)
[2] NeXT Satellite Proposal,the NeXT working group, submitted to ISAS/JAXA (2005)
[3] H. Kunieda, "Hard X-ray Telescope Mission (NeXT)" , Proc. SPIE, **5488**, 187 (2004)
[4] T. Takahashi, K. Mitsuda, & H. Kunieda, "The NeXT Mission" ,Proc. SPIE, **6266**, 62660D (2006)
[5] T. Takahashi et al., "The NeXT Mission", Proc. SPIE, **7011**, 70110O-1 (2008)
[6] T. Takahashi, K. Mitsuda, R.L. Kelley et al., "The ASTRO-H Mission", Proc. SPIE, **7732**, pp. 77320Z-77320Z-18 (2010)
[7] T. Takahashi, K. Mitsuda, R.L. Kelley et al., "The ASTRO-H Observatory", Proc. SPIE, **8443**, pp. 84431Z- 84431Z-22 (2012)
[8] T. Takahashi, K. Mitsuda, R.L. Kelley et al., "The ASTRO-H X-ray astronomy satellite", Proc. SPIE, **9114**, pp. 994125-914425-24 (2014)
[9] SXS Proposal, "High Resolution X-ray Spectroscopy for the JAXA New Exploration X-ray Telescope", NASA/GSFC, submitted to NASA (2007)
[10] K. Ishimura et al. "Novel Technique for Spacecraft's Thermal Deformation Test Based on Transient Phenomena", Transactions of the Japan Society for Aeronautical and Space Sciences, Aenrospace Technology Japan, **12** sits 29 (2014)
[11] T. Shimada et al., "Development Status of Electrical Power Subsystem for X-ray Astronomy Satellite ASTRO-H", IEICE Tech. Rep., **112**, no. 229, SANE2012-58, pp. 17-22, (2012)
[12] N. Iwata et al., "Thermal control system of x-ray astronomy satellite astro-h: Current development status and prospects," 44th International Conference on Environmental Systems (2014).
[13] N. Iwata et al., "JAXA's X-ray Astronomy Mission ASTRO-H: Launch and First Month's In-Orbit Thermal Performance," in *Proceedings of 46th International Conference on Environmental Systems*, in press (2016).
[14] L. Angelini et al., "ASTRO-H data analysis, processing and archive", Proc. SPIE **9905**, 9905-37 (2016).
[15] Hitomi collaboration, "The Quiet Intracluster Medium in the Core of the Perseus Cluster", Nature, 535, 117 (2016)
[16] L. Gallo et al., 'The Canadian ASTRO-H Metrology System", Proc. SPIE,**9144** (2014)
[17] T. Yuasa et al., "A Determinitic Spacewire Network Onboard The ASTRO-H Space X-ray Obseratory", Proceedings of International SpaceWire Conference", November 8-10, Texas, (2011)
[18] M.Kirsch et al.,"Crab: the standard x-ray candle with all (modern) x-ray satellites", Proc. SPIE. **5898**, 22 (2005)
[19] M. Tsujimoto et al., "Cross-calibration of the X-ray instruments onboard the Chandra, INTEGRAL, RXTE, Suzaku, Swift, and XMM-Newton observatories using G21.5-0.9", Astronomy and Astrophysics, **525**, A25 (2011)
[20] P.J.Serlemitsos et al., "The X-Ray Telescope onboard Suzaku", PASJ, 59, 9 (2007)
[21] T. Okajima et al., "Soft x-ray mirrors onboard the NeXT satellite", Proc. SPIE, **7011**, 85 (2008)

[22] P. Serlemitsos et al., "Foil x-ray mirrors for astronomical observations: still an evolving technology", Proc. SPIE **7732**, pp. 77320A-77320A-6 (2010)
[23] T. Okajima et al. "The first measurement of the ASTRO-H soft x-ray telescope performance", Proc. SPIE, **8443** (2012)
[24] Y. Soong et al. "ASTRO-H Soft X-ray telescope (SXT)", Proc. SPIE, **9144**, pp. 994128-914425-14 (2014)
[25] T. Okajima et al. " First Peak of ASTRO-H Soft X-ray Telescope (SXT) In-orbit Performance ", Proc. SPIE, **9905**9905-39 (2016)
[26] H. Kunieda et al., "Balloon-borne hard X-ray Imaging Observation of non-thermal
[27] Y. Ogasaka et al., "Thin-foil multilayer-supermirror hard x-ray telescopes for InFOCμS/SUMIT balloon experiments and NeXT satellite program", Proc. SPIE **6688**, 668803 (2007).
[28] F. Harrison et al., "Development of the High-Energy Focusing Telescope (HEFT) Balloon Experiment," Proc. SPIE, **4012**, 693 (2000)
[29] F. A. Harrison et al., "The Nuclear Spectroscopic Telescope Array (NuSTAR)," ApJ,**770**, 103 (2013)
[30] Y. Ogasaka et al., "The NeXT x-ray telescope system: status update", Proc. SPIE, **7011**, 70110P-1 (2008) phenomena", Proc. SPIE, **6266**, 62660B (2006)
[31] H. Kunieda, H. Awaki et al., "Hard X-ray Telescope to be onboard ASTRO-H", Proc. SPIE **7732**,pp. 773214-773214-12 (2010)
[32] H. Awaki et al., "Current status of ASTRO-H hard x-ray telescopes (HXTs)", Proc. SPIE, **8443**, 844324 (2012)
[33] H. Awaki et al., "ASTRO-H Hard X-ray telescope (HXT) ', Proc. SPIE, **9144**, 914426 (2014)
[34] H. Awaki et al., "The Hard X-ray Telescope to be onboard ASTRO-H", Appl. Opt. 53, pp. 7664-7676 (2014)
[35] H. Awaki et al., "Performance of ASTRO-H Hard X-ray Telescope (HXT)", Proc. SPIE, **9905** 9905-35 (2016)
[36] M. Nynka et al., "NuSTAR Study of Hard X-Ray Morphology and Spectroscopy of PWN G21.5-0.9," ApJ,**789**, 72 (2014)
[37] C. P. de Vries et al., "Calibration sources for the soft x-ray spectrometer instrument on ASTRO-H", Proc. SPIE, **8443** 844353 (2012)
[38] K. Mitsuda et al. "The X-ray microcalorimeter on the NeXT mission", Proc. SPIE, **7011**, 701102K-1 (2008)
[39] K. Mitsuda et al. "The high-resolution x-ray microcalorimeter spectrometer system for the SXS on ASTRO-H", Proc. SPIE, **7732** , pp.773211-773211-10 (2010)
[40] K. Mitsuda et al. "Soft x-ray spectrometer (SXS): the high-resolution cryogenic spectrometer onboard ASTRO-H", Proc. SPIE **9144**,pp. 773211-773211-10 (2014)
[41] R.L. Kelley et al.,"The ASTRO-H high-resolution soft x-ray spectrometer", Proc. SPIE, **9905** 9905-28 (2016)
[42] R.L. Kelley et al.,"The Suzaku High Resolution X-Ray Spectrometer", PASJ, **59**, pp.77-112 (2007)
[43] R.L. Kelley et al.,"Ion-implanted Silicon X-Ray Calorimeters: Present and Future",J. Low Tem Phys., **151**, Nos. 1-2 (2008)
[44] F. S. Porter and et al., "The detector subsystem for the SXS instrument on the ASTRO-H Observatory", Proc. SPIE **7732**, pp. 77323J-77323J-13 (2010)
[45] C. Kilbourne et al., "The design, implementation, and performance of the Atro-H SXS calorimeter array and anti-coincidence detector". Proc. SPIE, **9905** 9905-97(2016)
[46] P.J. Shirron et al. "Design and on-orbit operation of the adiabatic demagnetization refrigerator on the ASTRO-H soft x-ray spectrometer instrument", Proc. SPIE, **9905** 9905-105 (2016)
[47] R. Fujimoto et al., "Performance of the helium dewar and cryocoolers of ASTRO-H SXS". Proc. SPIE, **9905** 9905-104 (2016)
[48] Y. Takei et al., "Vibration isolation system for cryocoolers of Soft X-ray Spectrometer (SXS) onboard ASTRO-H (Hitomi)". Proc. SPIE, **9905** 9905-30 (2016)

[49] F. S. Porter et al., "In-flight performance of the soft x-ray spectrometer detector system on ASTRO-H". Proc. SPIE, **9905** 9905-29(2016)
[50] M. Tsujimoto et al., "In-orbit operation of the ASTRO-H SXS". Proc. SPIE, **9905** 9905-31 (2016)
[51] G. Sneiderman et al.,"Cryogen-free operation of the Soft X-ray Spectrometer instrument", Proc. SPIE **9905** , 9905-99 (2016)
[52] T. G. Tsuru et al., "Soft X-ray Imager (SXI) onboard the NeXT satellite", Proc. SPIE, **6266**, 62662I (2006)
[53] H. Tsunemi et al., "The SXI: CCD camera onboard the NeXT mission", Proc. SPIE, **7011**, 70110Q-1 (2008)
[54] H. Tsunemi et al., "The SXI: CCD camera onboard ASTRO-H", Proc. SPIE **7732**, pp. 773210-773210-11 (2010)
[55] H. Tsunemi et al., "Soft x-ray imager (SXI) onboard ASTRO-H", Proc. SPIE, **8443**, (2012)
[56] K. Hayashida et al., "Soft x-ray imager (SXI) onboard ASTRO-H", Proc. SPIE, **9144**, (2014)
[57] H. Tsunemi et al., "Soft x-ray imager (SXI) on-board ASTRO-H". Proc. SPIE, **9905** 9905-35 (2016)
[58] K. Koyama et al., "X-Ray Imaging Spectrometer (XIS) on Board Suzaku", PASJ, **59**, pp.23-33 (2007)
[59] T. Takahashi et al., "Wide band X-ray Imager (WXI) and Soft Gamma-ray Detector (SGD) for the NeXT Mission," Proc. SPIE, **5488**, p549-560 (2004)
[60] K. Nakazawa et al.,"Hard x-ray Imager for the NeXT Mission", Proc. SPIE, **6266**, 62662H (2006)
[61] M. Kokubun et al., "Hard x-ray imager (HXI) for the NeXT mission", Proc. SPIE, **7011**, 70110R-1 (2008)
[62] M. Kokubun et al., "Hard x-ray imager for the ASTRO-H Mission", Proc. SPIE **7732**, pp. 773215-773215-13 (2010)
[63] M. Kokubun et al., "Hard x-ray imager (HXI) for the ASTRO-H Mission", Proc. SPIE, **8443**, (2012)
[64] G. Sato et al., "The hard x-ray imager (HXI) for the ASTRO-H mission", Proc. SPIE, **9144**, (2014)
[65] G. Sato et al., "The Si/CdTe semiconductor camera of the ASTRO-H Hard X-ray Imager (HXI)", Nucl. Instr. Meth, in press (2016)
[66] K. Nakazawa et al.,"The hard x-ray imager (HXI) onboard ASTRO-H", Proc. SPIE **9905**, 9905-34 (2016).
[67] T. Takahashi et al., "Hard X-Ray Detector (HXD) on Board Suzaku", PASJ, **59**, pp.35-51 (2007)
[68] M. Kokubun et al., "In-Orbit Performance of the Hard X-Ray Detector on Board Suzaku", PASJ, 59, 53 (2007)
[69] T. Takahashi et al."Hard X-ray and Gamma-Ray Detectors for the NEXT mission", New Astronomy Reviews, 48, pp. 309-313 (2004)
[70] H. Tajima. et al.,"Soft Gamma-ray Detector for the ASTRO-H Mission", Proc. SPIE **7732**, pp. 773216-773216-17 (2010)
[71] S. Watanabe et al., "Soft gamma-ray detector for the ASTRO-H Mission", Proc. SPIE, **8443** (2012)
[72] Y. Fukazawa et al., "Soft gamma-ray detector for the ASTRO-H Mission", Proc. SPIE, **9144** , (2014)
[73] S. Watanabe et al. "The Si/CdTe semiconductor Compton camera of the ASTRO-H Soft Gamma-ray Detector (SGD)", Nucl. Instr. Meth. **765**, pp. 192-201 (2013)
[74] S. Watanabe et al.,"The soft gamma-ray detector (SGD) onboard ASTRO-H", Proc. SPIE **9905**, 9905-36 (2016).